CROATICA CHEMICA ACTA
CCACAA, ISSN 0011-1643, e-ISSN 1334-417X
Croat. Chem. Acta **86** (4) (2013) 453–462.
http://dx.doi.org/10.5562/cca2314

Original Scientific Article

Stability of Dimethylmercury and Related Mercury-containing Compounds with Respect to Selected Chemical Species Found in Aqueous Environment†

Laimutis Bytautas

Department of Chemistry, Rice University, Houston, Texas 77005, USA,
Present address: Galveston College, Department of Chemistry, 4015 Avenue Q, Galveston, TX, 77550, USA.
(E-mail: bytautas777@gmail.com)

RECEIVED JUNE 23, 2013; REVISED OCTOBER 3, 2013; ACCEPTED OCTOBER 4, 2013

Abstract. Dimethylmercury (CH_3−Hg−CH_3) and other Hg-containing compounds can be found in atmospheric and aqueous environments. These substances are highly toxic and pose a serious environmental and health hazard. Therefore, the understanding of chemical processes that affect the stability of these substances is of great interest. The mercury-containing compounds can be detected in atmosphere, as well as soil and aqueous environments where, in addition to water molecules, numerous ionic species are abundant. In this study we explore the stability of several small, Hg-containing compounds with respect to water molecules, hydronium (H_3O^+) ions as well as other small molecules/ions using density functional theory and wave function quantum chemistry methods. It is found that the stability of such molecules, most notably of dimethylmercury, can be strongly affected by the presence of the hydronium H_3O^+ ions. Although the present theoretical study represents gas phase results, it implies that pH level of a solution should be a major factor in determining the degree of abundance for dimethylmercury in aqueous environment. In particular, it is found that CH_3−Hg−CH_3 reacts readily with the H_3O^+ ion producing CH_3−Hg−OH_2^+ and methane indicating that *low-pH levels* favor the decomposition of dimethylmercury. On the other hand, our study suggests that *high-pH levels* in aqueous environment would favor strongly-bound complexes of [CH_3−Hg−CH_3•OH]$^-$ species. Overall, the theoretical evidence presented in this study offers an explanation for the available experimental data concerning the stability of dimethylmercury and other mercury-containing compounds having the general structure X−Hg−Y (X,Y = CH_3 and Cl) with respect to various ligands L (L = H_2O, NH_3, H_3O^+, OH^-, Cl^- and NH_4^+). (doi: 10.5562/cca2314)

Keywords: dimethylmercury, *ab initio* quantum chemistry, potential energy surfaces, toxicology, mercury-containing compounds

INTRODUCTION

Elemental mercury (Hg) is the only metal that is liquid at room temperature. This unique property evidently is related to relativistic effects.[1,2] Over many years mercury has been classified as a transition element (see *e.g.* Ref. 3), however recently this classification has been challenged. A recent paper by Jensen[4] suggests that Hg as well as Zn and Cd should not be classified as transition elements although some controversy still exists regarding this issue.[5,6] The ground state electronic configuration of mercury atom is [Xe] $4f^{14}$ $5d^{10}$ $6s^2$ indicating that the Hg-dimer should be a weakly bound van der Waals-type system in its ground state.[7]

Much attention has been dedicated to mercury-containing compounds containing halogens and methyl groups that are of practical significance to the human population. A large body of experimental data documenting effects of mercury to human health has accumulated over many years.[8–12] In this context, theoretical studies are important in elucidating possible chemical mechanisms involving Hg-containing species.[13] It is well known that mercury and its compounds, especially methylmercury species, *i.e.* compounds containing CH_3Hg-group, are extremely toxic to humans and other living organisms.[8–16] These compounds exist naturally in the environment, although human-related activities have contributed to the increased concentrations of mercury. It is understood that high affinity of the organomercurial compounds for thiols and lipophilic characteristics are the critical factors in their toxicity and various living organisms have developed unique neutralization mechanisms that counteract its effects. For example, bacteria developed two resistance pathways which involve the cleavage

† Dedicated to Professor Douglas Jay Klein on the occasion of his 70th birthday.

of Hg−C bond with a subsequent reduction of the mercuric residues to elemental mercury.[15,16] The presence of *methylmercurials* in soil, aqueous environment and the atmosphere is well documented.[17–27] Due to various transport mechanisms such compounds accumulate in living organisms, especially in aquatic environments. Methylmercury species are known[8] to cross the blood-brain barrier and are highly neurotoxic. One of the most toxic forms to humans among many mercury-containing chemical compounds is *dimethylmercury (DMHg)* with its chemical formula CH_3−Hg−CH_3. DMHg is a non-polar compound and readily accumulates in fatty tissues.[8,14] One of the important aspects in reducing the long-term exposure of methylmecury compounds to human population relates to understanding of chemical and physical processes controlling its concentration. Therefore, a significant volume of research has been dedicated to methylmercury, its demethylation as well as exploring other possible mechanisms involving mercury.[28–34] Evidently, DMHg is the predominant methylated form of mercury in the deep ocean.[23] It has been suggested[24] that the oceanic DMHg is the main source of monomethylmercury (MMHg) in the water column. The MMHg compound (*i.e.* methylmercury monocation $[CH_3–Hg]^+$) plays a significant role in the aqueous environment due to its ability to biomagnify in aquatic food chains leading to high toxicity levels in fish and other organisms. This seems to be the main pathway to the exposure of mercury to human population.[8,12] Recent findings of Conaway *et al.*[22] indicate unexpectedly high concentrations of DMHg in costal surface waters. Some studies[35] suggest that one possible route for the degradation of DMHg into MMHg in aqueous environments is by evaporating of DMHg into the atmosphere and, after the chemical transformation into MMHg, being brought back to the Ocean waters by aerosols or water vapor. An alternative route for the transformation from DMHg to MMHg may involve mechanisms and chemical species that can occur directly in aqueous environments.

A number of theoretical studies investigating chemistry of mercury-containing compounds have already been reported in the literature.[36–44] For example, mechanisms associated with the Hg−C bond cleavage by halogenic acids have been investigated by Barone and co-workers.[15] Ni *et al.*[36] investigated possible mechanisms for degrading chloromethylmercury (CH_3−Hg−Cl) and dimethylmercury (CH_3−Hg−CH_3) involving thiol and ammonium residues. Khalizov *et al.*[37] studied the reactions of Hg with halogens and discussed their atmospheric implications. Shepler *et al.*[38] have analyzed the effects of aqueous solvation on the thermochemistry of reactions between Hg and small halogen molecules. Furthermore, it has been proposed that organic mercury-containing compounds can be broken-down into less toxic species via photo-reduction and microbe-assisted transformations.[44,45] The role played by humic acids that are abundant in aqueous environment has been recently discussed in Ref. 20. A study by Tossell[44] examined the reaction energies for the formation of various CH_3−Hg−L species resulting from CH_3−Hg^+ and ligands L. In particular, Tossell's study[44] indicates that (CH_3−Hg−OH_2^+) should be the most dominant species in natural water systems.

Since methylmercury species frequently occur in aquatic environments, one of important questions is investigating the stability of these compounds with respect to exposure of water molecules as well as hydronium (H_3O^+) and hydroxide (OH^-) ions which, in turn are associated with pH levels of aqueous environments. Of particular interest is the observed *correlation between low pH levels and instability of DMHg.*[32–34] Thus, the goal of the present theoretical study is to explore possible mechanisms that can contribute to the chemical degradation of DMHg (CH_3−Hg−CH_3).

METHODOLOGY AND TECHNICAL DETAILS

The geometry optimizations in this study were performed for the following systems: H_2O, H_3O^+, OH^-, Cl^-, NH_4^+, CH_3−Hg−CH_3, CH_3−Hg−Cl, Cl−Hg−Cl, CH_3−Hg−OH_2^+. The ability of the Hg-containing compounds, *i.e.* CH_3−Hg−CH_3, CH_3−Hg−Cl and Cl−Hg−Cl to form complexes with the molecules of H_2O, H_3O^+, OH^-, Cl^-, NH_4^+ is explored by optimizing the geometries with the inclusion of the counterpoise correction (CP) to correct for the basis-set-superposition-error (BSSE).[46] The basis set used in all the calculations is 6-31G(d,p) (spherical harmonics) for all atoms except mercury. For the Hg atom the Stuttgart/Dresden pseudo-potential (effective-core-potential) MDF60 (see Refs. 47,48) was used to treat core electrons while the MWB60 basis set was used to treat valence electrons. The initial optimization step uses PBE DFT-functional and the resulting optimized geometry is used as the starting point in the MP2 optimization. After the geometry is optimized at the MP2 level of theory, a single-point CCSD(T) calculation is performed to obtain the total energy (electronic energy including nuclear repulsion). The vibrational analysis and the zero-point-energies correspond to the MP2 level of theory. All calculations were performed using GAUSSIAN package of *ab initio* programs.[49] Only local minima on the singlet ground-state potential energy surface[50–52] have been considered in this study.

RESULTS AND DISCUSSION

The strategy of this investigation is to explore possible complexes of the Hg-containing compounds, namely CH_3−Hg−CH_3, CH_3−Hg−Cl and Cl−Hg−Cl, with small

ligand molecules of H_2O, NH_3, CH_4 (neutral species) as well as ions of H_3O^+, OH^-, Cl^-, NH_4^+. As a first step, we calibrate our methods and basis sets against the benchmark data found in literature for selected molecular species to make sure that they are appropriate for the present investigation. *We note that the goal of the calibration step is not the quest for an extraordinary high accuracy (our chosen basis sets are too small for this purpose)* but rather to show that our final conclusions are expected to be reliable regarding the energetics of dissociation pathways of the Hg-containing compounds. We select Cl−Hg−Cl as our first case and compare our MP2 optimized geometry and vibrational frequencies with the previous high level calculations and experimental data.[53–55] The results are displayed in Table 1. As can be seen from the table the results of our MP2 optimization while not perfect yield quite satisfactory results. We also provide a comparison with experiment[56] of our MP2 optimized geometry for the CH_3−Hg−Cl compound in the supplementary material (see Table S1). The evidence supports that our level of theory and basis sets are capable of providing reliable results. To estimate the quality of our methodology on a weakly-bound neutral system we select the water dimer[57] as an example. We also consider the $H_5O_2^+$ molecule[58–61] as an example of a strongly-bound ionic system resulting from the interaction between the hydronium ion and water. We perform MP2 geometry optimizations for the water dimer and the $H_5O_2^+$ compound. Then, we calculate their dissociation energies (including the CP correction for BSSE) as described below. For the water dimer, the dissociation process is: $(H_2O{\bullet}H_2O) \rightarrow H_2O + H_2O$. For $H_5O_2^+$, the dissociation process is: $H_5O_2^+ \rightarrow H_2O + H_3O^+$. Of course, the calculation of these dissociation energies requires also MP2-geometry optimizations for H_2O and H_3O^+ structures. As seen in Table S1 of the supplementary material, our [MP2/6-31G(d,p)] value for the water-dimer dissociation energy of D_0 = 2.6 kcal/mol compares very well with the benchmark value of 2.88 kcal/mol of Ref. 57. The optimized geometries for the water dimer and $H_5O_2^+$ are displayed in Figure S1 (Figure S1A represents the water dimer geometry and Figure S1B represents that for the $H_5O_2^+$ molecule). For the $H_5O_2^+$ molecule, the data is displayed in Table S2 of the supplementary material. The geometry optimizations for $H_5O_2^+$ (with the counterpoise (CP) correction), H_3O^+ (without CP correction) and H_2O (without CP correction) have been performed at MP2 level of theory using 6-31G(d,p) basis set. The total electronic energies from MP2 and CCSD(T) calculations are reported in Table S2 of the supplementary material for each molecule (in hartree). The CCSD(T) energies have been calculated at the MP2-optimized geometries. Regarding the dissociation energy value D_e, it is evident that an agreement of the CCSD(T) result with the recent benchmark of Ref. 61 is excellent, the discrepancy being only 1.1 kcal/mol. The numerical data above clearly indicate that our selected theoretical methods and basis sets yield good-quality structures for *neutral* as well as *charged* molecular species that are relevant to the present study. Thus, it is expected that the following energies based on MP2-optimized geometries and CCSD(T) single-point energy calculations are reliable. Table S2 (see supplementary material) also lists the effect of zero-point-energies (ZPE) on the dissociation energy for the MP2 value (in parentheses). Next, we shall calculate the dissociation energies (without and with inclusion of ZPE) for bound complexes that involve *neutral* compounds CH_3−Hg−CH_3, CH_3−Hg−Cl and Cl−Hg−Cl with *neutral* species (ligands) of H_2O, NH_3 and CH_4 and examine their stability. Then, we obtain the binding energies of *neutral* compounds CH_3−Hg−CH_3, CH_3−Hg−Cl, Cl−Hg−Cl with *ionic* species of H_3O^+, OH^-, Cl^- and NH_4^+. Finally, we shall discuss the energetics and thermochemistry of these cases and draw our conclusions regarding the stability and most favorable decomposition pathways for the mercury-containing species, namely CH_3−Hg−CH_3, CH_3−Hg−Cl and Cl−Hg−Cl in aqueous environments.

X−Hg−Y Interaction with Neutral Ligands L (L = H_2O and NH_3)

The interaction and binding strength between X−Hg−Y and any of the neutral ligands L (L= H_2O or NH_3) where each symbol, X and Y, represents either CH_3-group or Cl-atom, has been calculated in an analogous manner as discussed above. The geometry of the NH_3 molecule is displayed in Figure S2 (panel A) of the supplementary material. The total electronic energies are then used for calculating energy differences to obtain binding electronic energies ΔE. In order to account for ZPE effects due to molecular vibrations, one must correct ΔE value by adding ZPE differences between reacting species, thus obtaining (ΔE+ΔZPE) value as ZPE-adjusted binding energy. In our notation, $\Delta E = -D_e$ and ΔE(ZPE) = $-D_0$.

The computational data documenting the interaction of X−Hg−Y species with neutral ligands L is listed in Table 2. The energetics for the complex formation as well as Gibbs free energy change and equilibrium constants are displayed in the table for X−Hg−Y complexes, namely CH_3−Hg−CH_3, CH_3−Hg−Cl, Cl−Hg−Cl that form with the H_2O molecule (rows I to III) and [CH_3−Hg−$CH_3{\bullet}NH_3$] (row IV). From Table 2 it is evident that the magnitude of binding energy, ΔE and ΔE(ZPE), steadily increases going from [CH_3−Hg−$CH_3{\bullet}H_2O$] to [CH_3−Hg−Cl$\bullet H_2O$] and to [Cl−Hg−Cl$\bullet H_2O$] as the total number of electronegative ligands L increases from (L = two CH_3 groups) to (L = one CH_3 and Cl) to (L = two Cl ligands), respectively.

Table 1. Bond distances (Å) and harmonic frequencies (cm^{-1}) for the geometry of Cl−Hg−Cl, the electronic state is $^1\Sigma_g^+$ ($D_{\infty h}$)

	This work [a]	Theory (Balabanov-Peterson) [b]		Experiment
		CBS [c]	CBS+CV+SR [d]	
		Geometry		
	2.2905	2.2509	2.2447	
		Harmonic Frequencies		**Fundamental Frequencies**
2, π_u	92	102	104	100 [e]
σ_g	350	363	367	360 [f]
σ_u	407	417	420	413 [f]

[a] The data based on MP2-optimized structure, see text.
[b] See paper by Balabanov and Peterson.[53]
[c] The results based on CCSD(T)/complete-basis-set equilibrium geometry.
[d] The results based on CCSD(T)/complete-basis-set equilibrium geometry with core-valence-correlations and scalar-relativistic effects being included.
[e] Ref. 54.
[f] Ref. 55.

Table 2. Complexes resulting from X−Hg−Y interaction with selected *neutral* Ligands (L): X−Hg−Y + L → [X−Hg−Y • L].
Reported results include energy differences based on electronic total energies, zero-point-energy (ZPE) corrected values as well as Gibbs free energy change ($\Delta G°$) of complex formation (298.15 K and 1 atm). Results correspond to CCSD(T) level of theory unless noted otherwise

	Complex Formation	ΔE[a] / kcal mol^{-1}	ΔE(ZPE)[b] / kcal mol^{-1}	$\Delta G°$ / kcal mol^{-1}	K [c]
I.	CH_3−Hg−CH_3 + H_2O → CH_3−Hg−CH_3 • H_2O	−1.74	−1.15	2.55	0.014
II.	Cl−Hg−CH_3 + H_2O → Cl−Hg−CH_3 • H_2O	−4.66	−3.58	0.88	0.226
III.	Cl−Hg−Cl + H_2O → Cl−Hg−Cl • H_2O	−6.58	−5.64	−0.70	3.259
IV.	CH_3−Hg−CH_3 + NH_3 → CH_3−Hg−CH_3 • NH_3	−2.28	−1.57	2.15	0.027

[a] ΔE is CCSD(T) energy difference between a complex [X−Hg−Y • L] and individual fragments, X−Hg−Y and L.
[b] ΔE value corrected for zero-point-energy effects. See supplementary material (Tables S1 and S2) for more information.
[c] Equilibrium constant [$K = \exp(-\Delta G°/RT)$] for the indicated reaction.

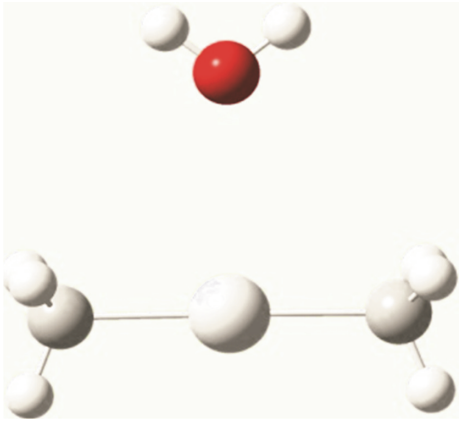

(A) CH_3−Hg−CH_3 • H_2O

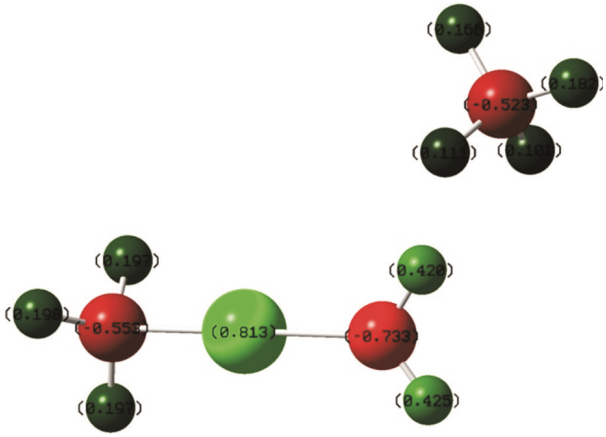

(B) PRODUCT FROM:
CH_3−Hg−CH_3 + H_3O^+ → $[CH_3$−Hg−$OH_2]^+$ • CH_4

Figure 1. The bound complexes resulting from the interaction of CH_3−Hg−CH_3 with H_2O (panel A) and H_3O^+ (panel B). In panel B the product of a barrier-less reaction: CH_3−Hg−CH_3 + H_3O^+ → $[CH_3$−Hg−OH_2•CH_4 $]^+$ is displayed.

It is to be expected that as the electron density from the central Hg atom in X−Hg−Y is withdrawn towards the electronegative ligand (chlorine) the binding of H_2O to X−Hg−Y gets stronger. Figures 1, 2 and 3 (panels A) clearly illustrate this trend. Finally, from Table 2 one can see that the binding energy for $[CH_3$−Hg−CH_3•$NH_3]$ is slightly larger than that in $[CH_3$−Hg−CH_3•$H_2O]$ (see Figure 4, panel A) which could be rationalized on the basis of larger basicity of NH_3 relative to H_2O.

X−Hg−Y interaction with ionic ligands L (L = H_3O^+, OH^-, Cl^- and NH_4^+)

Now, we shall examine the interaction and binding energy between X−Hg−Y and any of the ionic ligands L (L = H_3O^+, OH^-, Cl^- and NH_4^+) where each symbol, X and Y, represents either CH_3-group or Cl-atom. The

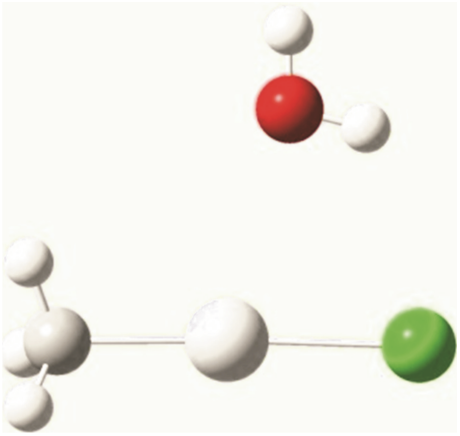

(A) CH_3−Hg−Cl • H_2O

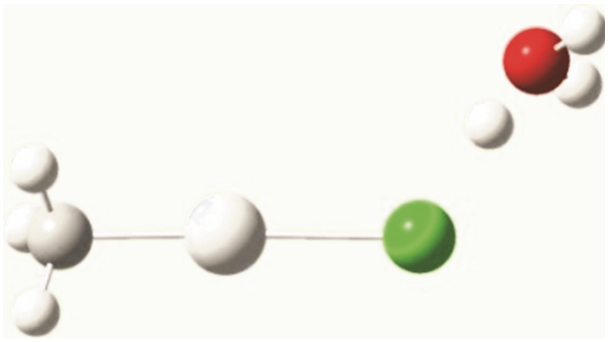

(B) CH_3−Hg−Cl • H_3O^+

Figure 2. The bound complexes resulting from the interaction of CH_3−Hg−Cl with H_2O (panel A) and H_3O^+ (panel B).

calculations follow the same procedure as discussed in the preceding section. The optimized geometry for NH_4^+ is displayed in Figure S2 (panel B) of the supplementary material. The relevant data is displayed in Table 3. The display of the contents in these tables is analogous to that of Table 2. Table 3 lists the data of interaction of $(CH_3$−Hg−$CH_3)$ with ions H_3O^+, OH^-, Cl^- and NH_4^+. From this table it is evident that the binding energy for $[CH_3$−Hg−CH_3•$NH_4]^+$ (see Figure 4-panel B), $[CH_3$−Hg−CH_3•$Cl]^-$ (see Figure 5) and $[CH_3$−Hg−CH_3•$OH]^-$ (see Figure 6) increases as the *bound ligand L* changes from NH_4^+ to Cl^- and then to OH^-. Since the concentration of OH^- ions in aqueous solution is a measure of pOH value, it is expected that *basic solutions* will favor the reduction of dimethyl-mercury concentration by producing strongly bound $[CH_3$−Hg−CH_3•$OH]^-$.

Next, we examine the reaction of dimethylmercury with the hydronium ion. The relevant data is listed in the first row of Table 3. The MP2 optimization starting with $(CH_3$−Hg−$CH_3)$ and H_3O^+ molecules placed at a short distance apart (ranging from about 3 Å to 6 Å from the Hg atom to H_3O^+) indicates that the

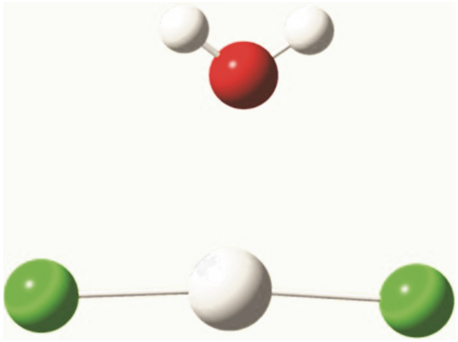

(A) Cl−Hg−Cl • H_2O

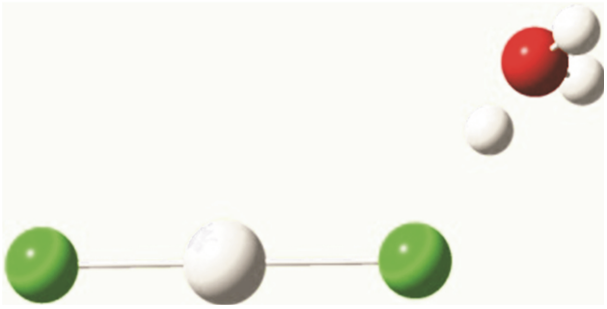

(B) Cl−Hg−Cl • H_3O^+

Figure 3. The bound complexes resulting from the interaction of Cl−Hg−Cl with H_2O (panel A) and H_3O^+ (panel B).

$[CH_3{-}Hg{-}CH_3{\bullet}H_3O]^+$ system decomposes readily without a barrier into $[CH_3{-}Hg{-}OH_2]^+$ and methane (see Figure 1, panel B). This result can be easily understood if we consider various decomposition fragments of the combined system, *i.e.* $CH_3{-}Hg{-}CH_3$ and H_3O^+. In Table 4 such different fragments are labeled as System-I, System-II and System-III. It is clearly evident that the System-III containing $[CH_3{-}Hg{-}OH_2]^+$ and methane (CH_4) as sum of two individual (non-interacting) fragments *is by far the most stable*, *i.e.* has the lowest electronic energy among them. Furthermore, there seems to be no barrier that could prevent the original system, *i.e.* $[CH_3{-}Hg{-}CH_3]$ plus H_3O^+, from ending up in this potential energy minimum. It may be noted that the absence of the energy barrier does not negate the existence of a transition state which can be determined on the basis of other considerations, *e.g.*, minimum flux using variational transition state theory[62,63] (see also Refs. 64,65). As a follow up investigation we performed an MP2 optimization for a weakly-bound complex $[CH_3{-}Hg{-}OH_2{\bullet}CH_4]^+$ which is labeled as System-IV in Table 4. It is found that this complex has nearly negligible binding energy of only 1.4 kcal/mol. The geometry of this complex is displayed in Figure 1 (panel B) where the Mulliken charges are also listed. The large positive charge exhibited by the mercury atom

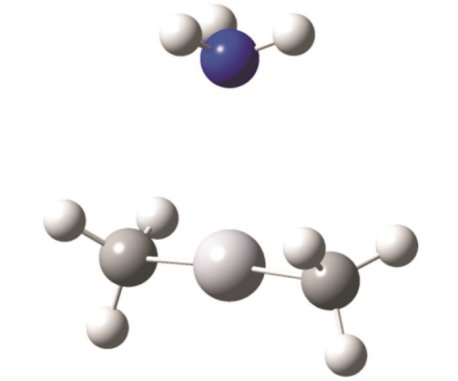

(A) CH_3-Hg-CH_3 • NH_3

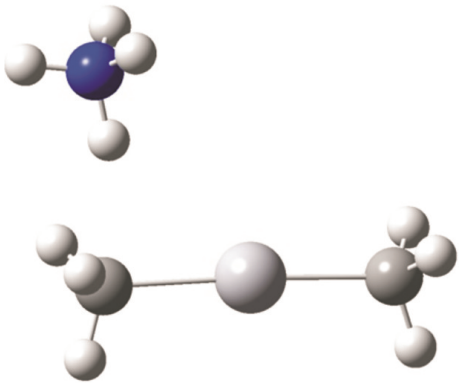

(B) $[CH_3$-Hg-$CH_3{\bullet}NH_4]^+$

Figure 4. The bound complexes resulting from the interaction of CH_3-Hg-CH_3 with NH_3 (panel A) and NH_4^+ (panel B).

is indicative of its cationic character that is commonly found in X−Hg−Y structures including some stable biomolecular complexes like T−Hg−T[66] where T = thymine.

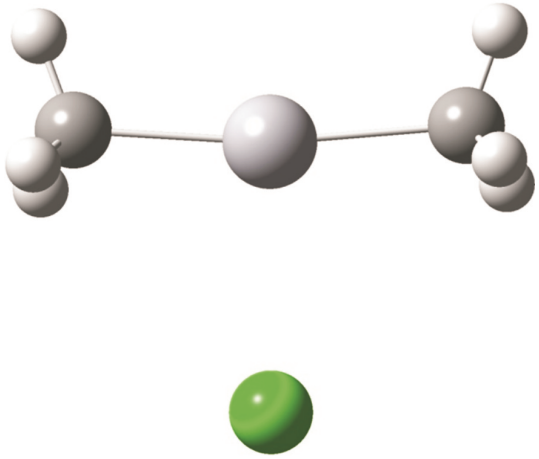

Figure 5. Optimized geometry for the $[CH_3{-}Hg{-}CH_3{\bullet}Cl]^{\square}$ ionic complex.

Table 3. Complexes resulting from $CH_3{-}Hg{-}CH_3$ interaction with selected *ionic* Ligands. Reported results include energy differences ΔE based on electronic total energies (with nuclear-nuclear repulsion), zero-point-energy (ZPE) corrected values as well as Gibbs free energy change ($\Delta G°$) of complex formation (298.15 K and 1 atm). The counterpoise correction has been applied unless noted otherwise

	Complex Formation	ΔE[(a)] / kcal mol^{-1}	ΔE(ZPE)[(b)] / kcal mol^{-1}	$\Delta G°$ / kcal mol^{-1}	K[(c)]
I.	$CH_3{-}Hg{-}CH_3 + H_3O^+ \rightarrow [CH_3{-}Hg{-}OH_2 \bullet CH_4]^+$	−59.62	−59.17	−57.35	1.091×10^{42}
II.	$CH_3{-}Hg{-}CH_3 + OH^- \rightarrow [CH_3{-}Hg{-}CH_3 \bullet OH^-]$	−27.31	−25.99	−19.87	3.671×10^{14}
III.	$CH_3{-}Hg{-}CH_3 + Cl^- \rightarrow [CH_3{-}Hg{-}CH_3 \bullet Cl^-]$	−12.05	−13.09	−8.58	1.946×10^{6}
IV.	$CH_3{-}Hg{-}CH_3 + NH_4^+ \rightarrow [CH_3{-}Hg{-}CH_3 \bullet NH_4]^+$	−6.13	−5.46	0.63	0.345

(a) ΔE is CCSD(T) energy difference between a bound [$CH_3{-}Hg{-}CH_3$•Ligand] system and individual fragments, $CH_3{-}Hg{-}CH_3$ and Ligand.
(b) ΔE value corrected for zero-point-energy effects. See supplementary material for more information (Tables S3 and S4).
(c) Equilibrium constant [$K = \exp(-\Delta G°/RT)$] for the indicated reaction.

Table 4. $CH_3{-}Hg{-}CH_3$ interaction with H_3O^+. The data correspond to various decomposition fragments resulting from $CH_3{-}Hg{-}CH_3$ and H_3O^+ interaction. The values for system-II and system-III are reported relative to the corresponding values of system-I. No counterpoise (CP) correction has been applied unless noted otherwise

	System	ΔE[(a)] / kcal mol^{-1}	ΔE(ZPE)[(b)] / kcal mol^{-1}	$\Delta G°$ / kcal mol^{-1}
I.	($CH_3{-}Hg{-}CH_3$ and H_3O^+)	0	0	0
II.	($[CH_3{-}Hg]^+$ and CH_4 and H_2O)	−17.77	−20.13	−27.91
III.	($[CH_3{-}Hg{-}OH_2]^+$ and CH_4)	−57.09	−57.49	−58.71

	Complex Formation[(c)]	ΔE[(a)] / kcal mol^{-1}	ΔE(ZPE)[(b)] / kcal mol^{-1}	$\Delta G°$ / kcal mol^{-1}	K[(d)]
IV.	$[CH_3{-}Hg{-}OH_2]^+ + CH_4 \rightarrow [CH_3{-}Hg{-}OH_2 \bullet CH_4]^+$	−2.27	−1.42	1.63	0.064

(a) ΔE corresponds to the CCSD(T) level of theory.
(b) ΔE value corrected for zero-point-energy effects. See supplementary material for more information (Table S4).
(c) $[CH_3{-}Hg{-}OH_2 \bullet CH_4]^+$: CP-corrected for Basis-set-superposition error (BSSE). See supplementary material for more information (Table S4).
(d) Equilibrium constant [$K = \exp(-\Delta G°/RT)$] for the indicated reaction (298.15 K and 1 atm).

Table 5. Hydronium ion interaction with X−Hg−Y. Total energies at CCSD(T) level of theory and zero-point energies at MP2 level of theory

	Complex Formation	ΔE[(a)] / kcal mol^{-1}	ΔE(ZPE)[(b)] / kcal mol^{-1}	$\Delta G°$ / kcal mol^{-1}	K[(c)]
I.	$CH_3{-}Hg{-}CH_3 + H_3O^+ \rightarrow [CH_3{-}Hg{-}OH_2 \bullet CH_4]^+$	−59.62	−59.17	−57.35	1.091×10^{42}
II.	$CH_3{-}Hg{-}Cl + H_3O^+ \rightarrow [CH_3{-}Hg{-}Cl \bullet H_3O]^+$	−27.76	−27.68	-[(d)]	-[(d)]
III.	$Cl{-}Hg{-}Cl + H_3O^+ \rightarrow [Cl{-}Hg{-}Cl \bullet H_3O]^+$	−16.19	−15.64	-[(d)]	-[(d)]
IV.	$Cl{-}Hg{-}Cl + H_5O_2^+ \rightarrow [Cl{-}Hg{-}Cl \bullet H_5O_2]^+$	−9.80	−8.59	−1.99	28.753

(a) ΔE is CCSD(T) energy difference between a bound [X−Hg−Y • L] system and individual fragments, X−Hg−Y and L. In case of System-I:ΔE is CCSD(T) energy difference between $[CH_3{-}Hg{-}OH_2{\bullet}CH_4]^+$ and fragments $CH_3{-}Hg{-}CH_3$ and H_3O^+.
(b) ΔE value corrected for zero-point-energy effects. See supplementary material for more information (Tables S5 and S6).
(c) Equilibrium constant [$K = \exp(-\Delta G°/RT)$] for the indicated reaction (298.15 K and 1 atm).
(d) Data not available.

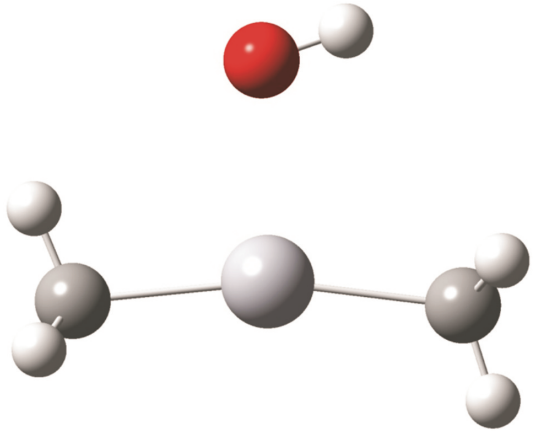

Figure 6. Optimized geometry for the $[CH_3{-}Hg{-}CH_3{\bullet}OH]^{+}$ ionic complex.

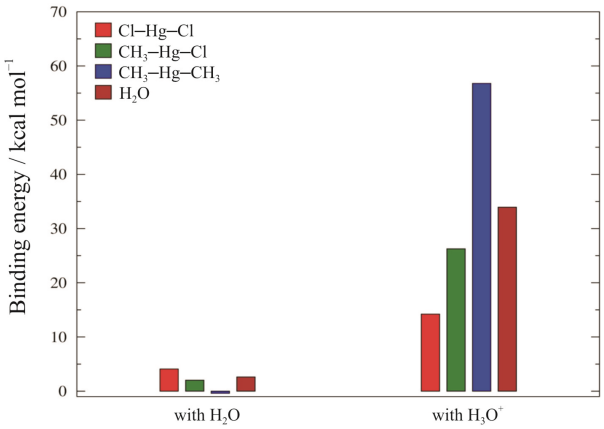

Figure 7. Comparison of binding energies (see text) of the selected mercury-containing species (X−Hg−Y) with ligands L (L = H_2O and H_3O^+).

Finally, in Table 5 we compare binding energies of the *hydronium ion* with all three X−Hg−Y structures, namely [$CH_3{-}Hg{-}CH_3$ plus H_3O^+], [$CH_3{-}Hg{-}Cl$ plus H_3O^+] and [$Cl{-}Hg{-}Cl$ plus H_3O^+] that are labeled as System-I, System-II and System-III, respectively. From Table 5 it is evident that the binding energy increases going from [$Cl{-}Hg{-}Cl{\bullet}H_3O^+$] (see Figure 3-panel B) to [$CH_3{-}Hg{-}Cl{\bullet}H_3O^+$] (see Figure 2-panel B) and to [$CH_3{-}Hg{-}CH_3$ plus H_3O^+] (see Figure 1-panel B). The reaction of $CH_3{-}Hg{-}CH_3$ with H_3O^+ produces a much more stable complex $[CH_3{-}Hg{-}OH_2{\bullet}CH_4]^+$. This trend in binding energies is also displayed graphically in Figure 7. While the reaction $CH_3{-}Hg{-}CH_3 + H_3O^+ \rightarrow CH_3{-}Hg{-}OH_2^+ + CH_4$ is spontaneous and has a large equilibrium constant at room temperature, the reaction $CH_3{-}Hg{-}CH_3 + H_2O \rightarrow CH_3{-}Hg{-}OH + CH_4$ would require higher temperatures to produce noticeable concentrations of the products. Also, the fourth row (labeled system-IV) in Table 5 provides the data for complex formation of $[Cl{-}Hg{-}Cl \bullet H_5O_2]^+$ as shown in Figure 8 (panel-B).

Discussion

The goal of the present theoretical study is to explore possible mechanisms that can contribute to the chemical degradation of DMHg ($CH_3{-}Hg{-}CH_3$). Furthermore, we also explore additional Hg-containing compounds, namely $Cl{-}Hg{-}Cl$ and $CH_3{-}Hg{-}Cl$, focusing on their binding strength with respect to water and hydronium ions as well as ions of OH^-, Cl^- and NH_4^+. The present work examines energetics and thermochemistry of degradation pathways of X−Hg−Y complexes (here, each symbol X and Y represents either CH_3 or Cl). As noted earlier, the present theoretical work is primarily focused on the exploration of the interaction of ($CH_3{-}Hg{-}CH_3$) with *water molecules and hydronium ions* which relates closely with pH levels and the stability of DMHg in aqueous environments. The current work shows that the DMHg is *highly unstable* with respect to H_3O^+ and decomposes readily while the presence of other ions, like OH^-, Cl^- and NH_4^+, has a somewhat weaker effect on the stability of DMHg. Although the present study corresponds to gas-phase conditions, the instability of DMHg with respect to the hydronium ion clearly implies that in aqueous environment the rate of degradation of DMHg should increase as value of pH gets smaller. Manifestly, our result is in accord with the experimental observations regarding the dependence of increased instability of DMHg with lower pH levels in

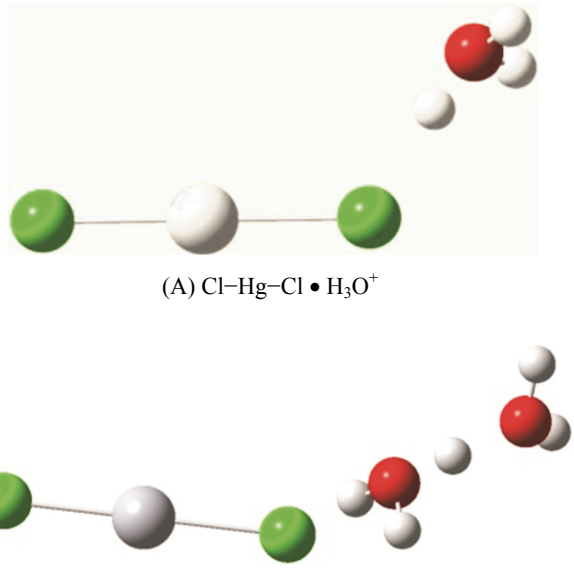

(A) $Cl{-}Hg{-}Cl \bullet H_3O^+$

(B) $Cl{-}Hg{-}Cl \bullet H_5O_2^+$

Figure 8. Comparison of the bound complexes resulting from the interaction of $Cl{-}Hg{-}Cl$ with H_3O^+ (panel A) and $H_5O_2^+$ (panel B).

aqueous environment found in literature.[32–34] We also demonstrate that Cl−Hg−CH_3 which has only one methyl group is much more stable with respect to the hydronium ion as compared to the DMHg compound. This result correlates well with a recent report by Korbas *et al.*[14] which suggests that dimethylmercury should be more susceptible to C−Hg protonolysis than monomethyl species based solely on the examination of the distribution of Mulliken atomic charges. Manifestly, the data above sheds some light regarding the rapid demethylation of dimethylmercury to monomethyl species reported by Ostlund[27] in his laboratory experiments. Our conclusion regarding the instability of DMHg with respect to H_3O^+ which proceeds without a detectable barrier to yield the products $[CH_3{-}Hg{-}OH_2]^+$ and CH_4, correlates closely with the result of Ni *et al.*[37] who found that, in the gas phase, backside protonolysis of the Hg−C bond of $[CH_3Hg(SH)_2]^-$ by the ammonium ion (NH_4^+) occurs without a detectable barrier as well.

CONCLUSIONS

The goal of the present investigation is to explore the stability of several mercury-containing compounds of the general form X−Hg−Y (X = CH_3, Cl and Y = CH_3, Cl) with respect to several small molecules which we call ligands L for simplicity that are frequently found in aqueous environments. We consider a set of neutral ligands (L=H_2O or NH_3) and a set of charged ligands (L= H_3O^+, OH^-, Cl^- and NH_4^+). We find that, in general, *ionic ligands* form *much more strongly bound* complexes with X−Hg−Y compounds of the form $[X{-}Hg{-}Y{\bullet}L]^q$ compared to their neutral counterparts (here q indicates the electric charge of the complex). The largest energy lowering was found for $CH_3{-}Hg{-}CH_3 + OH^- \rightarrow [CH_3{-}Hg{-}CH_3 \bullet OH]^-$ and $CH_3{-}Hg{-}CH_3 + H_3O^+ \rightarrow CH_3{-}Hg{-}OH_2^+ + CH_4$ reactions with large equilibrium constants at room temperature in both cases. The weakly bound-complex $[CH_3{-}Hg{-}OH_2{\bullet}CH_4]^+$ has the binding energy of only 1.4 kcal/mol with respect to the dissociation fragments $[CH_3{-}Hg{-}OH_2]^+$ and CH_4 that is 59.2 kcal/mol lower than the [$CH_3{-}Hg{-}CH_3$ plus H_3O^+] system. The $[CH_3{-}Hg{-}CH_3{\bullet}OH]^-$ complex is 26.0 kcal/mol lower than the system composed of non-interacting fragments $CH_3{-}Hg{-}CH_3$ and OH^-.

Overall, our study indicates that dimethylmercury is unstable in low-pH aquatic environments readily decomposing into $[CH_3{-}Hg{-}OH_2]^+$ and CH_4. This work provides the quantitative data for explaining the experimental observations reporting that *low-pH levels of aqueous medium favor a rapid decomposition of* $CH_3{-}Hg{-}CH_3$ (see Refs. 32–34). Our result is in accord with the earlier findings by Tossell who noted the remarkable stability of $[CH_3{-}Hg{-}OH_2]^+$ compound in water systems in his earlier investigations[44] of photo-decomposition of methyl Hg complexes. On the other hand, our study shows *that high-pH levels* in aqueous environment would favor strongly-bound complexes of $[CH_3{-}Hg{-}CH_3{\bullet}OH]^-$ species.

Supplementary Materials. – Supporting informations to the paper are enclosed to the electronic version of the article. These data can be found on the website of *Croatica Chemica Acta* (http://public.carnet.hr/ccacaa).

Acknowledgements. This work is dedicated to Professor Douglas J. Klein (on the occasion of his 70-th birthday) whom the author has had a great pleasure of knowing for many years. During this time, the author has been impressed by Professor Klein's scientific originality and depth in solving numerous problems in chemistry, physics and mathematics of remarkable diversity. The author has no doubt that many significant breakthrough research papers authored by Professor Klein will appear in scientific literature in the near future. The author has a great appreciation to Professor Klein for his role as a mentor during the author's early scientific carrier. The author acknowledges useful discussions with Professor Gustavo E. Scuseria, Dr. Kousik Samanta and Dr. Carlos Jiménez-Hoyos.

REFERENCES

1. P. Pyykkö, *Ann. Rev. Phys. Chem.* **63** (2012) 45.
2. L. J. Norrby, *J. Chem. Ed.* **68** (1991) 110.
3. M. D. Morse, *Chem. Rev.* **86** (1986) 1049.
4. W. B. Jensen, *J. Chem. Ed.* **80** (2003) 952.
5. W. B. Jensen, *J. Chem. Ed.* **85** (2008) 1182.
6. X. F. Wang, L. Andrews, S. Riedel, and M. Kaupp, *Angew. Chem. Int. Ed.* **46** (2007) 8371.
7. E. Pahl, D. Figgen, C. Thierfelder, K. A. Peterson, F. Calvo, and P. Schwerdtfeger, *J. Chem. Phys.* **132** (2010) 114301.
8. M. H. Keating, *Mercury Study Report to Congress, Vol. 1: Executive Summary*, United States Environmental Protection Agency, 1997.
9. T. W. Clarkson and L. Magos, *Crit. Rev. Toxicol.* **36** (2006) 609.
10. R. A. Goyer, *Toxological effects of Methylmercury*, National Academy Press: Washington DC, **2000**.
11. H. H. Harris, I. J. Pickering, and N. G. Graham, *Science* **301** (2003) 1203.
12. D. Mergler, H. A. Anderson, L. H. M. Chan, K. R. Mahaffey, M. Murray, M. Sakamoto, and A. H. Stern, *Ambio* **36** (2007) 3.
13. D. Cremer, E. Kraka, and M. Filatov, *ChemPhysChem* **9** (2008) 2510.
14. M. Korbas, J. L. O'Donoghue, G. E. Watson, I. J. Pickering, S. P. Singh, G. J. Myers, T. W. Clarkson, and G. N. George, *ACS Chem. Neurosci.* **1** (2010) 810.
15. V. Barone, A. Bencini, F. Totti, and M. G. Uytterhoeven, *Organometalics* **15** (1995) 1465.
16. M. J. Moore, M. D. Distefano, L. D. Zydowski, R. T. Cummings, and W. T. Walsh, *Acc. Chem. Res.* **23** (1990) 301.
17. G. Topping and I. M. Davies, *Nature* **290** (1981) 243.
18. I. Lehnherr, V. L. St. Louis, H. Hintelmann, and J. L. Kirk, *Nature Geoscience* **4** (2011) 298.
19. J. J. Alberts, J. E. Schindler, R. W. Miller, and D. E. Nutter Jr., *Science* **184** (1974) 895.
20. B. Gu, Y. Bian, C. L. Miller, W. Dong, X. Jiang, and L. Liang, *Proc. Nat. Acad. Sciences (USA)* **108** (2011) 1479.
21. A. Bollen and H. Biester, *Water Air Soil Pollut.* **219** (2011) 175.

22. C. H. Conaway, F. J. Black, M. Gault-Ringold, J. T. Pennington, F. P. Chavez, and A. R. Flegal, *Environ. Sci. Technol.* **43** (2009) 1305.
23. W. F. Fitzgerald, C. H. Lamborg, and C. R. Hammerschmidt, *Chem. Rev.* **107** (2007) 641.
24. R. P. Mason and W. F. Fitzgerald, *Deep Sea Res. Part I* **40** (1993) 1897.
25. N. M. Lawson and R. P. Mason, *Biogeochemistry* **40** (1998) 235.
26. R. Pongratz and K. G. Heuman, *Chemosphere* **39** (1999) 89.
27. K. Ostlund, *Acta Pharmacol. Toxicol.* **27** (Suppl) (1969) 1.
28. J. Mink and B. Gellai, *J. Organomet. Chem.* **66** (1974) 1.
29. A. M. W. Bakke, *J. Mol. Spectrosc.* **41** (1972) 1.
30. R. E. Rebbert and P. Ausloos, *J. Am. Chem. Soc.* **85** (1963) 3086.
31. H. Niki, P. D. Maker, C. M. Savage, and L. P. Breitenbach, *J. Phys. Chem.* **87** (1983) 4978.
32. N. L. Wolfe, R. G. Zepp, J. A. Gordon, and G. L. Baughman, *Chemosphere* **2** (1972) 147.
33. T. Fagerström and A. Jernelöv, *Water Research* **6** (1972) 1193.
34. M. R. Winfrey and J. W. M. Rudd, *Environ. Toxicol. Chem.* **9** (1990) 853.
35. C. J. Lin and S. O. Pehkonen, *Atmos. Environ.* **33** (1999) 2067.
36. B. Ni, J. R. Kramer, R. A. Bell, and N. H. Werstiuk, *J. Phys. Chem. A* **110** (2006) 9451.
37. A. F. Khalizov, B. Viswanathan, P. Larregaray, and P. Ariya, *J. Phys. Chem. A* **107** (2003) 6360.
38. B. C. Shepler, A. D. Wright, N. B. Balabanov, and K. A. Peterson, *J. Phys. Chem. A* **111** (2007) 11342.
39. H.-C. Tai and C. Lim, *J. Phys. Chem. A* **110** (2006) 452.
40. X. Li, R.-Z. Liao, W. Zhou, and G. Chen, *Phys. Chem. Chem. Phys.* **12** (2010) 3961.
41. L. Castro, A. Dommergue, A. Renard, C. Ferrari, A. Ramirez-Solis, and L. Maron, *Phys. Chem. Chem. Phys.* **13** (2011) 16772.
42. D. Majumdar, S. Rosak, and J. Leszczynski, *Chem. Phys. Lett.* **501** (2011) 308.
43. A. T. Afaneh, G. Schereckenbach, and F. Wang, *Theor. Chem. Acc.* **131** (2012) 1174.
44. J. A. Tossell, *J. Phys. Chem. A* **102** (1998) 3587.
45. P. Sellers, S. A. Kelley, J. W. M. Rudd, and A. R. Mac-Hutchon, *Nature* **380** (1996) 694.
46. S. F. Boys and F. Bernardi, *Mol. Phys.* **19** (1970) 553.
47. www.theochem.uni-stuttgart.de/pseudopotentials/
48. D. Figgen, G. Rauhut, M. Dolg, and H. Stoll, *Chem. Phys.* **311** (2005) 227.
49. M. J. Frisch, G. W. Trucks, H. B. Schlegel, G. E. Scuseria, M. A. Robb, J. R. Cheeseman, G. Scalmani, V. Barone, et al. Gaussian 09, Revision A.02; Gaussian Inc.: Wallingford CT, 2009.
50. L. Bytautas, J. M. Bowman, X. Huang, and A.J.C. Varandas, *Adv. Phys. Chem.* **2012** (2012) 679869.
51. L. Bytautas, "*Theoretical Studies of Chemical Reactions*", Ph. D. Thesis, Vanderbilt University, Nashville, TN, USA (1996).
52. H. B. Schlegel, *J. Comp. Chem.* **24** (2003) 1514.
53. N. B. Balabanov and K. A. Peterson, *J. Chem. Phys.* **119** (2003) 12271.
54. B. J. Aylett, *Comprehensive Inorganic Chemistry*, Pergamon Press: Elmsford, NY, 1973, Vol. 3.
55. D. M. Adams and D. J. Hills, *J. Chem. Soc. Dalton Trans.* (1978) 776.
56. W. Gordy, J. Sheridan, *J. Chem. Phys.* **22** (1954) 92.
57. M. W. Feyereisen, D. Feller, and D. A. Dixon, *J. Phys. Chem.* **100** (1996) 2993.
58. J. M. Headrick, E.G. Dicken, R. S. Walters, N. I. Hammer, R. A. Christie, J. Cui, E. M. Myshakin, M. A. Duncan, M. A. Johnson, and K. D. Jordan, *Science* **308** (2005) 1765.
59. T. L. Guasco, M. A. Johnson, and A. B. McCoy, *J. Phys. Chem. A* **115** (2011) 5847.
60. S. G. Olesen, T. L. Guasco, J. R. Roscioli, and M. A. Johnson, *Chem. Phys. Lett.* **509** (2011) 89.
61. X. Huang, B. J. Braams, and J. M. Bowman, *J. Chem. Phys.* **122** (2005) 044308.
62. D. G. Truhlar and B. C. Garrett, *Acc. Chem. Res.* **13** (1980) 440.
63. D. G. Truhlar, B. C. Garrett, and S. J. Klippenstein, *J. Phys. Chem.* **100** (1996) 12771.
64. R. E. Stanton and J. W. McIver Jr., *J. Am. Chem. Soc.* **97** (1975) 3632.
65. L. Bytautas and D. J. Klein, *Int. J. Quantum Chem.* **70** (1998) 205.
66. T. Uchiyama, T. Miura, H. Takeuchi, T. Dairaku, T. Komuro, T. Kawamura, Y. Kondo, L. Benda, V. Sychrovský, P. Bouř, I. Okamoto, A. Ono, and Y. Tanaka, *Nucleic Acids Res.* **40** (2012) 5766.

SUPPLEMENTAL MATERIAL

Stability of dimethylmercury and related mercury-containing compounds with respect to selected chemical species found in aqueous environment

Laimutis Bytautas

Department of Chemistry, Rice University, Houston, Texas 77005, USA [a-c)]

[a)] Present address: Galveston College, Department of Chemistry, 4015 Avenue Q, Galveston, TX, 77550, USA.
[b)] Email: bytautas777@gmail.com
[c)] This work is dedicated to Professor Douglas J. Klein on the occasion of his 70-th birthday.

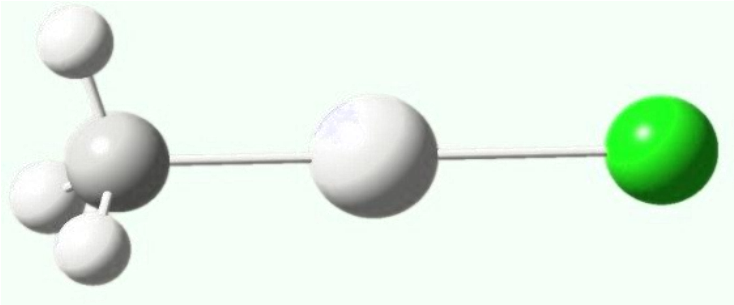

Table SI. Comparison between calculated and experimental[a)] bond distances (in Å) and angles (in degree) for the optimized geometries CH_3-Hg-Cl.

Geometry	PBE	MP2	Experiment
r(Hg-Cl)	2.331	2.327	2.282
r(Hg-C)	2.075	2.075	2.061
angle(C-Hg-Cl)	180.0	180.0	180.0

[a)] Experimental data represents pure rotational spectra (see ref. [56]).

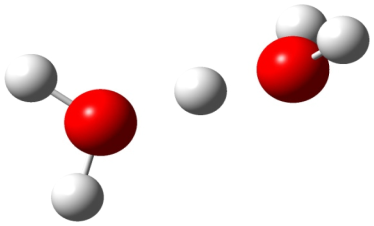

Table SII. Comparison of results [a] obtained by methods used in the present study (6-31G(d,p) basis sets) to the benchmark literature value for the dissociation energy (D_e) of $H_5O_2^+$. Total electronic energies are listed in hartree while dissociation energies are listed in kcal/mol.

Method	$H_5O_2^+$ (hartree)	H_3O^+ (hartree)	H_2O (hartree)	$H_5O_2^+ \rightarrow H_2O + H_3O^+$ (kcal/mol)
MP2	-152.778980 [b]	-76.503724	-76.217280	36.38
CCSD(T)	-152.802585 [b]	-76.517393	-76.229123	35.18
Benchmark [d] (ref. [61])				**34.09**

[a] MP2-optimized geometry, see text.
[b] CP-corrected electronic energy values.
[c] CCSD(T) level of theory result using aug-cc-pVTZ basis sets.

TABLE SIII. H_2O interaction with X-Hg-Y. Total electronic energies at CCSD(T) level of theory, zero-point-energies (ZPE) and Gibbs free energies (298.15 K and 1 atm) at MP2 level of theory. Energy units are in hartree.

System Level-of-theory	Energy CCSD(T)	ZPE-correction MP2	G^0-correction MP2	E(ZPE) [a]	G^0
I. CH_3–Hg–CH_3 • H_2O	**-308.452 295** [b]	**0.096 440**	**0.055 878**	**-308.355855**	**-308.396417**
CH_3–Hg–CH_3	-232.220 407	0.073 621	0.044 808		
H_2O	-76.229 123	0.021 886	0.004 241		
Sum	**-308.449 530**	**0.095 507**	**0.049049**	**-308.354023**	**-308.400481**
II. Cl–Hg–CH_3 • H_2O	**-728.344 271** [c]	**0.061 906**	**0.022 871**	**-728.282 365**	**-728.321400**
Cl–Hg–CH_3	-652.107 714	0.038 287	0.009 798		
H_2O	-76.229 123	0.021 886	0.004 241		
Sum	**-728.336 837**	**0.060 173**	**0.014039**	**-728.276 664**	**-728.322798**
III. Cl–Hg–Cl • H_2O	**-1148.213 561** [d]	**0.025 537**	**-0.011722**	**-1148.188 024**	**-1148.225283**
Cl–Hg–Cl	-1071.973 951	0.002 146	-0.025339		
H_2O	-76.229 123	0.021 886	0.004241		
Sum	**-1148.203 074**	**0.024 032**	**-0.021098**	**-1148.179 042**	**-1148.224172**

[a] E(ZPE) is the total energy value to which the ZPE is added.
[b] System-I: CP-corrected for Basis-set-superposition error (BSSE) = 5.205 mh (millihartree).
[c] System-II: CP-corrected for Basis-set-superposition error (BSSE) = 6.432 mh.
[d] System-III: CP-corrected for Basis-set-superposition error (BSSE) = 7.770 mh.

Table SIV. Interaction of CH_3–Hg–CH_3 with NH_3 and H_2O. Total energies at CCSD(T) level of theory, zero-point energies and Gibbs free energies (298.15 K and 1 atm) at MP2 level of theory. The counterpoise (CP) correction has been applied.

System Level-of-theory	Energy CCSD(T)	ZPE MP2	G^0-correction MP2	E(ZPE) [a]	G^0 (free energy)
CH_3–Hg–CH_3 • NH_3	**-288.624 053** [b]	**0.110 216**	**0.069312**	**-288.513837**	**-288.554741**
CH_3–Hg–CH_3	-232.220 407	0.073 621	0.044808		
NH_3	-56.400 009	0.035 466	0.017442		
Sum	**-288.620 416**	**0.109 087**	**0.062250**	**-288.511329**	**-288.558166**

[a] E(ZPE) is the total energy value to which the ZPE is added.

[b] CP-corrected for Basis-set-superposition error (BSSE) = 5.286 mh.

Table SV. Complexes resulting from CH_3–Hg–CH_3 interaction with selected ionic Ligands. Reported results include energy differences based on electronic total energies, the zero-point-energy (ZPE) corrected values as well as Gibbs free energy change of complex formation (T=298.15 K and 1 atm). The counterpoise correction has been applied.

System Level-of-theory	Total Energy CCSD(T)/hartree	ZPE MP2/hartree	G^0 MP2/hartree	ΔE[a)] millihartree	$\Delta E(ZPE)$[b)] millihartree	ΔG^0 millihartree
I. $[CH_3–Hg–CH_3 \bullet OH]^-$	**-307.795 063** [c)]	**0.084 098**	**0.048 759**	**-43.523**	**-41.419**	**-31.672**
$CH_3–Hg–CH_3$	-232.220 407	0.073 621	0.044808			
OH^-	-75.531 144	0.008 373	-0.007900			
Sum	**-307.751 540**	**0.081 994**	**0.036908**			
II. $[CH_3–Hg–CH_3 \bullet Cl]^-$	**-691.903 163** [d)]	**0.071 959**	**0.034664**	**-19.203**	**-20.865**	**-13.667**
$CH_3–Hg–CH_3$	-232.220 407	0.073 621	0.044808			
Cl^-	459.663 564	0.0	-0.015680			
Sum	**-691.883 960**	**0.073 621**	**0.029128**			
III. $[CH_3–Hg–CH_3 \bullet NH_4]^+$	**-288.982 493** [e)]	**0.125 568**	**0.086803**	**-9.762**	**-8.697**	**0.997**
$CH_3–Hg–CH_3$	-232.220 407	0.073 621	0.044808			
NH_4^+	-56.752 324	0.050 882	0.031236			
Sum	**-288.972 731**	**0.124 503**	**0.076044**			

a) ΔE is CCSD(T) energy difference between a bound [CH_3–Hg–CH_3•Ligand] system and individual fragments, CH_3–Hg–CH_3 and Ligand.
b) $\Delta E(ZPE)$ represents ΔE with an additional correction due to ZPE.
c) System-I: CP-corrected for Basis-set-superposition error (BSSE) = 54. 186 mh.
d) System-II: CP-corrected for Basis-set-superposition error (BSSE) = 13.812 mh.
e) System-III: CP-corrected for Basis-set-superposition error (BSSE) = 1.821 mh.

Table SVI. CH_3–Hg–CH_3 interaction with selected ionic Ligands. Total energies at CCSD(T) level of theory and zero-point energies at MP2 level of theory for various decomposition fragments resulting from CH_3–Hg–CH_3 and H_3O^+ interaction. No counterpoise (CP) correction has been applied unless noted otherwise.

System Level-of-theory	Total Energy CCSD(T)/hartree	ZPE MP2/hartree	G^0 MP2/hartree	ΔE[a)] millihartree	$\Delta E(ZPE)$[b)] millihartree	ΔG^0 millihartree
I. CH_3–Hg–CH_3	-232.220 407	0.073 621	0.044808			
H_3O^+	-76.517 394	0.035 287	0.016154			
Sum	**-308.737 801**	**0.108 908**	**0.060962**	**0.0**	**0.0**	**0.0**
II. $[CH_3–Hg]^+$	-192.148 639	0.036 718	0.011323			
CH_4	-40.388 354	0.046 537	0.029234			
H_2O	-76.229 124	0.021 886	0.004241			
Sum	**-308.766 116**	**0.105 141**	**0.044798**	**-28.315**	**-32.082**	**-44.479**
III. $[CH_3–Hg–OH_2]^+$	-268.440 425	0.061 736	0.029141			
CH_4	-40.388 354	0.046 537	0.029234			
Sum	**-308.828779**	**0.108 273**	**0.058375**	**-90.978**	**-91.613**	**-93.565**

System Level-of-theory	Total Energy CCSD(T)/hartree	ZPE MP2/hartree	G^0 MP2/hartree	ΔE[a)] millihartree	$\Delta E(ZPE)$[b)] millihartree	ΔG^0 millihartree
IV. $[CH_3–Hg–OH_2•CH_4]^+$	**-308.832 815** [d)]	**0.109 636**	**0.064586**	**-3.619**	**-2.256**	**2.592**
V. The geometries taken from System-IV and ZPEs for $[CH_3–Hg–OH_2]^+$ and CH_4 taken from System-III)						
$[CH_3–Hg–OH_2]^+$	-268.440 302	0.061 736	0.029141			
CH_4	-40.388 894	0.046 537	0.029234			
Sum:	**-308.829 196**	**0.108 273**	**0.058375**	**0.0**	**0.0**	**0.0**

a) ΔE is CCSD(T) energy with respect to the energy of System-I.

b) $\Delta E(ZPE)$ represents an additional correction to ΔE that is due to ZPE.

c) ΔE is CCSD(T) energy difference between a bound [CH_3–Hg–CH_3 • Ligand] system and individual fragments, CH_3–Hg–CH_3 and Ligand.

d) System-IV: CP-corrected for Basis-set-superposition error (BSSE) = 1.312 mh.

Table SVII. Hydronium ion interaction with X-Hg-Y. Total energies at CCSD(T) level of theory and zero-point energies at MP2 level of theory.

System Level-of-theory	Total Energy CCSD(T)/hartree	ZPE MP2/hartree	G^0 MP2/hartree	ΔE[a)] millihartree	$\Delta E(ZPE)$[b)] millihartree	ΔG^0
I. $[CH_3–Hg–OH_2•CH_4]^+$	**-308.832 815** [c)]	**0.109 636**	**0.064586**	**-95.014**	**-94.286**	**-91.39**
$CH_3–Hg–CH_3$	-232.220 407	0.073 621	0.044808			
H_3O^+	-76.517 394	0.035 287	0.016154			
Sum	**-308.737 801**	**0.108 908**	**0.060962**			
II. $[CH_3–Hg–Cl• H_3O]^+$	**-728.669 346** [d)]	**0.073 697**	**-**	**-44.238**	**-44.115**	
$CH_3–Hg–Cl$	-652.107 714	0.038 287				
H_3O^+	-76.517 394	0.035 287				
Sum	**-728.625 108**	**0.073 574**				
III. $[Cl–Hg–Cl•H_3O]^+$	**-1148.517 143** [e)]	**0.038 306**	**-**	**-25.798**	**-24.925**	
$Cl–Hg–Cl$	-1071.973 951	0.002 146				
H_3O^+	-76.517 394	0.035 287				
Sum	**-1148.491 345**	**0.037 433**				

a) ΔE is CCSD(T) energy difference between a bound $[X–Hg–Y • H_3O^+]$ system and individual fragments, X–Hg–Y and H_3O^+. In case of System-I: ΔE is CCSD(T) energy difference between $[CH_3–Hg–OH_2•CH_4]^+$ and fragments $CH_3–Hg–CH_3$ and H_3O^+.

b) $\Delta E(ZPE)$ represents ΔE with an additional correction due to ZPE.

c) System-I: CP-corrected for Basis-set-superposition error (BSSE) = 1.312 mh with respect to $[CH_3–Hg–OH_2]^+$ and CH_4.

d) System-II: CP-corrected for Basis-set-superposition error (BSSE) = 4.056 mh.

e) System-III: CP-corrected for Basis-set-superposition error (BSSE) = 3.393 mh.

Table SVIII. $H_5O_2^+$ interaction with Cl-Hg-Cl. Total energies at CCSD(T) level of theory and zero-point energies at MP2 level of theory.

System Level-of-theory	Total Energy CCSD(T)/hartree	ZPE MP2/hartree	G^0 MP2/hartree	ΔE[a)] millihartree	$\Delta E(ZPE)$[b)] millihartree	ΔG^0 millihartree
Cl–Hg–Cl + $H_5O_2^+$ → $[Cl–Hg–Cl \bullet H_5O_2]^+$				**-15.624**	**-13.697**	**-3.174**
$[Cl–Hg–Cl \bullet H_5O_2]^+$	**-1224.796844**	**0.063165**	**0.021444**			
Cl-Hg-Cl	**-1071.973951**	**0.002146**	**-0.025339**			
$H_5O_2^+$	**-152.807269**	**0.059092**	**0.034333**			
Sum:	**-1224.781220**	**0.061238**	**0.008994**			

a) ΔE is CCSD(T) energy difference between a bound $[X–Hg–Y\bullet H_5O_2]^+$ system and individual fragments, Cl–Hg–Cl and $H_5O_2^+$.

b) $\Delta E(ZPE)$ represents ΔE with an additional correction due to ZPE.

Table SIX. $[CH_3–Hg–OH_2• CH_4]^+$ geometry optimization with counterpoise-correction.

MP2-optimization:

```
Symbolic Z-matrix:
 Charge =  1 Multiplicity = 1 in supermolecule
 Charge =  0 Multiplicity = 1 in fragment  1.
 Charge =  1 Multiplicity = 1 in fragment  2.
```

STARTING

Hg(Fragment=2)	-0.44744	-0.07157	-0.00113
C(Fragment=1)	4.11396	0.87291	-0.00632
H(Fragment=1)	5.07513	1.37196	0.06143
H(Fragment=1)	4.20986	0.07108	-0.73732
H(Fragment=1)	3.36951	1.59586	-0.33047
C(Fragment=2)	-2.2601	0.93097	-0.00034
H(Fragment=2)	-2.54015	1.08328	1.03802
H(Fragment=2)	-2.10698	1.87356	-0.51789
H(Fragment=2)	-2.9752	0.30022	-0.52067
O(Fragment=2)	1.47853	-1.14155	0.04772
H(Fragment=2)	1.60169	-2.05802	-0.24027
H(Fragment=1)	3.87093	0.48574	0.98203
H(Fragment=2)	2.33866	-0.68933	0.01382

MP2 result:

Counterpoise: corrected energy = -308.767627465143

Counterpoise: BSSE energy = 0.001224163545

Rotating derivatives to standard orientation.

	1	2	3
	A	A	A
Frequencies --	1.3486	7.8742	21.1059
Red. masses --	1.0288	1.0498	3.4207
Frc consts --	0.0000	0.0000	0.0009
IR Inten --	0.1071	0.0766	0.7629

	4	5	6
	A	A	A
Frequencies --	71.6342	95.2669	115.0029
Red. masses --	1.1291	2.7031	3.7041
Frc consts --	0.0034	0.0145	0.0289
IR Inten --	0.1175	1.1816	2.7644

	7	8	9
	A	A	A
Frequencies --	138.5207	149.5043	161.3586
Red. masses --	2.0177	1.4947	1.0318

Frc consts --	0.0228	0.0197	0.0158
IR Inten --	34.7510	69.1961	7.5999

	10	11	12
	A	A	A
Frequencies --	314.6155	364.7499	543.2254
Red. masses --	1.0934	5.7526	4.7164
Frc consts --	0.0638	0.4509	0.8200
IR Inten --	182.0657	31.1515	0.9375

	13	14	15
	A	A	A
Frequencies --	646.9352	884.7238	886.6558
Red. masses --	1.1078	1.1475	1.1508
Frc consts --	0.2732	0.5292	0.5331
IR Inten --	35.5620	23.1034	29.6996

	16	17	18
	A	A	A
Frequencies --	1292.3146	1372.1477	1410.2110
Red. masses --	1.1623	1.1731	1.1773
Frc consts --	1.1437	1.3014	1.3794
IR Inten --	46.4470	24.3354	16.2301

	19	20	21
	A	A	A
Frequencies --	1419.6683	1490.4616	1490.7089
Red. masses --	1.1718	1.0600	1.0601
Frc consts --	1.3915	1.3874	1.3879
IR Inten --	17.8598	2.4160	2.2191

	22	23	24
	A	A	A
Frequencies --	1618.8943	1621.9223	1670.7442
Red. masses --	1.0135	1.0086	1.0822
Frc consts --	1.5650	1.5632	1.7798
IR Inten --	14.0957	5.1863	35.8161

	25	26	27
	A	A	A
Frequencies --	3112.4241	3158.5061	3245.8319
Red. masses --	1.0093	1.0258	1.1035
Frc consts --	5.7606	6.0292	6.8496
IR Inten --	17.4547	4.1817	14.7532

	28	29	30
	A	A	A
Frequencies --	3259.7253	3286.3679	3293.4976
Red. masses --	1.1016	1.1000	1.1081
Frc consts --	6.8964	6.9998	7.0817
IR Inten --	14.5748	2.2163	4.7845

	31	32	33
	A	A	A
Frequencies --	3294.3066	3772.5523	3912.0090

```
 Red. masses --     1.1083                1.0468                1.0824
 Frc consts  --     7.0863                8.7780                9.7601
 IR Inten    --     4.5357              426.5748              349.8526


 -------------------
 - Thermochemistry -
 -------------------
 Temperature   298.150 Kelvin.  Pressure   1.00000 Atm.
 Atom     1 has atomic number 80 and mass 201.97060
 Atom     2 has atomic number  6 and mass  12.00000
 Atom     3 has atomic number  1 and mass   1.00783
 Atom     4 has atomic number  1 and mass   1.00783
 Atom     5 has atomic number  1 and mass   1.00783
 Atom     6 has atomic number  6 and mass  12.00000
 Atom     7 has atomic number  1 and mass   1.00783
 Atom     8 has atomic number  1 and mass   1.00783
 Atom     9 has atomic number  1 and mass   1.00783
 Atom    10 has atomic number  8 and mass  15.99491
 Atom    11 has atomic number  1 and mass   1.00783
 Atom    12 has atomic number  1 and mass   1.00783
 Atom    13 has atomic number  1 and mass   1.00783
 Molecular mass:   251.03594 amu.
 Principal axes and moments of inertia in atomic units:
                           1         2         3
     Eigenvalues --   210.16925 1562.39724 1748.61365
           X            0.99999   0.00405  -0.00112
           Y           -0.00404   0.99995   0.00862
           Z            0.00116  -0.00861   0.99996
 This molecule is an asymmetric top.

Warning -- explicit consideration of  12 degrees of freedom as
           vibrations may cause significant error
 Vibrational temperatures:      1.94    11.33    30.37   103.07   137.07
          (Kelvin)            165.46   199.30   215.10   232.16   452.66
                              524.79   781.58   930.79  1272.92  1275.70
                             1859.35  1974.21  2028.98  2042.58  2144.44
                             2144.79  2329.22  2333.58  2403.83  4478.08
                             4544.38  4670.02  4690.01  4728.34  4738.60
                             4739.77  5427.85  5628.50


 Zero-point correction=                           0.109636 (Hartree/Particle)
 Thermal correction to Energy=                    0.120649
 Thermal correction to Enthalpy=                  0.121593
 Thermal correction to Gibbs Free Energy=         0.064586
 Sum of electronic and zero-point Energies=           -308.657991
 Sum of electronic and thermal Energies=              -308.646978
 Sum of electronic and thermal Enthalpies=            -308.646034
 Sum of electronic and thermal Free Energies=         -308.703041
```

CCSD(T) Result:

```
 Charge =  1 Multiplicity = 1 in supermolecule
 Charge =  0 Multiplicity = 1 in fragment  1.
 Charge =  1 Multiplicity = 1 in fragment  2.
```

Hg(Fragment=2)	-0.447374871763	-0.071538640553	-0.000795572863 H
C(Fragment=1)	4.113842935478	0.872852541269	-0.006764954566 H
H(Fragment=1)	5.075083232272	1.371858888813	0.060284320396 H
H(Fragment=1)	4.208947069786	0.071508399258	-0.738312227837 H
H(Fragment=1)	3.369108973985	1.595972765468	-0.329665515444 H
C(Fragment=2)	-2.259937654143	0.931171200420	-0.000530255848 H
H(Fragment=2)	-2.540241427735	1.083584291917	1.037720068701 H
H(Fragment=2)	-2.106608039117	1.873698523643	-0.518091538514 H
H(Fragment=2)	-2.974952951914	0.300470340683	-0.520995587284 H
O(Fragment=2)	1.478497515278	-1.141659694130	0.048593238151 H
H(Fragment=2)	1.601551609374	-2.058360658928	-0.238693686276 H
H(Fragment=1)	3.871821191647	0.485088252278	0.981560455568 H
H(Fragment=2)	2.338662417024	-0.689536210779	0.014297254615 H

CCSD(T) Result:

Counterpoise: corrected energy = -308.832814709825

Counterpoise: BSSE energy = 0.001311946240

Table SXX. The data for MP2-geometry optimization of CH_3–Hg – CH_3 .

```
--------------------------------------------------------------------------------------------------
-- Stationary point found.

                          ! (Angstroms and Degrees)  !
 --------------------------                          --------------------------
 ! Name  Definition              Value          Derivative Info.                !
 --------------------------------------------------------------------------------
 ! R1    R(1,2)                  2.1045         -DE/DX =    0.0                 !
 ! R2    R(1,6)                  2.1045         -DE/DX =    0.0                 !
 ! R3    R(2,3)                  1.0897         -DE/DX =    0.0                 !
 ! R4    R(2,4)                  1.0897         -DE/DX =    0.0                 !
 ! R5    R(2,5)                  1.0897         -DE/DX =    0.0                 !
 ! R6    R(6,7)                  1.0897         -DE/DX =    0.0                 !
 ! R7    R(6,8)                  1.0897         -DE/DX =    0.0                 !
 ! R8    R(6,9)                  1.0897         -DE/DX =    0.0                 !
 ! A1    A(1,2,3)              110.6778         -DE/DX =    0.0                 !
 ! A2    A(1,2,4)              110.6778         -DE/DX =    0.0                 !
 ! A3    A(1,2,5)              110.6778         -DE/DX =    0.0                 !
 ! A4    A(3,2,4)              108.2382         -DE/DX =    0.0                 !
 ! A5    A(3,2,5)              108.2382         -DE/DX =    0.0                 !
 ! A6    A(4,2,5)              108.2382         -DE/DX =    0.0                 !
 ! A7    A(1,6,7)              110.6778         -DE/DX =    0.0                 !
 ! A8    A(1,6,8)              110.6778         -DE/DX =    0.0                 !
 ! A9    A(1,6,9)              110.6778         -DE/DX =    0.0                 !
 ! A10   A(7,6,8)              108.2382         -DE/DX =    0.0                 !
 ! A11   A(7,6,9)              108.2382         -DE/DX =    0.0                 !
 ! A12   A(8,6,9)              108.2382         -DE/DX =    0.0                 !
 ! A13   L(2,1,6,4,-1)         180.0            -DE/DX =    0.0                 !
 ! A14   L(2,1,6,4,-2)         180.0            -DE/DX =    0.0                 !
 ! D1    D(3,2,6,7)            120.0063         -DE/DX =    0.0                 !
 ! D2    D(3,2,6,8)           -119.9937         -DE/DX =    0.0                 !
 ! D3    D(3,2,6,9)              0.0063         -DE/DX =    0.0                 !
 ! D4    D(4,2,6,7)           -119.9937         -DE/DX =    0.0                 !
 ! D5    D(4,2,6,8)              0.0063         -DE/DX =    0.0                 !
 ! D6    D(4,2,6,9)            120.0063         -DE/DX =    0.0                 !
 ! D7    D(5,2,6,7)              0.0063         -DE/DX =    0.0                 !
 ! D8    D(5,2,6,8)            120.0063         -DE/DX =    0.0                 !
 ! D9    D(5,2,6,9)           -119.9937         -DE/DX =    0.0                 !
 --------------------------------------------------------------------------------
 GradGradGradGradGradGradGradGradGradGradGradGradGradGradGradGradGradGrad

      E2 =    -0.4602618546D+00 EUMP2 =    -0.23217016021166D+03

                 The electronic state is 1-A1.

Harmonic frequencies (cm**-1), IR intensities (KM/Mole), Raman scattering
 activities (A**4/AMU), depolarization ratios for plane and unpolarized
 incident light, reduced masses (AMU), force constants (mDyne/A),
 and normal coordinates:
                      1                      2                      3
                     A1                     E                      E
 Frequencies --    42.6016              145.1571              145.1571
 Red. masses --     1.0078                2.7828                2.7828
 Frc consts  --     0.0011                0.0345                0.0345
 IR Inten    --     0.0000                0.0449                0.0449

                      4                      5                      6
                     A1                     A2                     E
 Frequencies --   527.3465              552.0616              726.3182
 Red. masses --     3.9904                4.0984                1.1443
 Frc consts  --     0.6538                0.7359                0.3557
 IR Inten    --     0.0000               44.5414                0.0000
```

```
                     7                      8                      9
                     E                      E                      E
 Frequencies --    726.3182               826.7602               826.7602
 Red. masses --      1.1443                 1.2346                 1.2346
 Frc consts  --      0.3557                 0.4972                 0.4972
 IR Inten    --      0.0000                38.6836                38.6836

                     10                     11                     12
                     A1                     A2                     E
 Frequencies --   1289.9141              1290.3531              1505.3280
 Red. masses --      1.1788                 1.2174                 1.0598
 Frc consts  --      1.1556                 1.1943                 1.4149
 IR Inten    --      0.0000                 1.8609                 0.0000

                     13                     14                     15
                     E                      E                      E
 Frequencies --   1505.3280              1508.9551              1508.9551
 Red. masses --      1.0598                 1.0531                 1.0531
 Frc consts  --      1.4149                 1.4127                 1.4127
 IR Inten    --      0.0000                 0.5768                 0.5768

                     16                     17                     18
                     A2                     A1                     E
 Frequencies --   3129.5558              3129.8848              3232.2459
 Red. masses --      1.0325                 1.0321                 1.1014
 Frc consts  --      5.9578                 5.9573                 6.7794
 IR Inten    --     20.1189                 0.0000                 0.0000


                     19                     20                     21
                     E                      E                      E
 Frequencies --   3232.2459              3232.3250              3232.3250
 Red. masses --      1.1014                 1.1022                 1.1022
 Frc consts  --      6.7794                 6.7851                 6.7851
 IR Inten    --      0.0000                25.2909                25.2909


 -------------------
 - Thermochemistry -
 -------------------
 Temperature   298.150 Kelvin.  Pressure   1.00000 Atm.
 Atom     1 has atomic number 80 and mass 201.97060
 Atom     2 has atomic number  6 and mass  12.00000
 Atom     3 has atomic number  1 and mass   1.00783
 Atom     4 has atomic number  1 and mass   1.00783
 Atom     5 has atomic number  1 and mass   1.00783
 Atom     6 has atomic number  6 and mass  12.00000
 Atom     7 has atomic number  1 and mass   1.00783
 Atom     8 has atomic number  1 and mass   1.00783
 Atom     9 has atomic number  1 and mass   1.00783
 Molecular mass:   232.01755 amu.

Warning -- explicit consideration of   5 degrees of freedom as
           vibrations may cause significant error
 Vibrational temperatures:     61.29   208.85   208.85   758.73   794.29
          (Kelvin)           1045.01  1045.01  1189.52  1189.52  1855.90
```

```
                          1856.53  2165.83  2165.83  2171.05  2171.05
                          4502.73  4503.20  4650.48  4650.48  4650.59
                          4650.59

 Zero-point correction=                           0.073621 (Hartree/Particle)
 Thermal correction to Energy=                    0.079390
 Thermal correction to Enthalpy=                  0.080334
 Thermal correction to Gibbs Free Energy=         0.044808
 Sum of electronic and zero-point Energies=          -232.096539
 Sum of electronic and thermal Energies=             -232.090770
 Sum of electronic and thermal Enthalpies=           -232.089826
 Sum of electronic and thermal Free Energies=        -232.125352

-------------------------------------------------------------------------------

 ---------------------------------------------------------------
 #P CCSD-T(FC,MaxCyc=100) SCF(Tight) CHKbasis GEOM=allcheck
 ---------------------------------------------------------------

               CCSD(T)= -0.23222040714D+03

State=1-A1\HF=-231.7098984\MP2=-232.1701602\MP3=-23
 2.1939366\MP4D=-232.2057569\MP4DQ=-232.2001924\MP4SDQ=-232.2063701\CCS
 D=-232.2053395\CCSD(T)=-232.2204071\
===============================================================================
```

Table SXXI. The data for MP2-geometry optimization of CH_3–Hg^+.

```
 ---------------------------------------------------------------------
 # MP2 CHKbasis Opt(CalcFC,Tight,MaxCycle=150,MaxStep=30) Freq GEOM=all
 check
 ---------------------------------------------------------------------

E2 =    -0.2760510826D+00 EUMP2 =    -0.19211663732637D+03

The electronic state is 1-A1.

Harmonic frequencies (cm**-1), IR intensities (KM/Mole), Raman scattering
 activities (A**4/AMU), depolarization ratios for plane and unpolarized
 incident light, reduced masses (AMU), force constants (mDyne/A),
 and normal coordinates:
                      1                      2                      3
                     A1                     E                      E
 Frequencies --   439.4440               851.8637               851.8637
 Red. masses --     5.0979                 1.0940                 1.0940
 Frc consts  --     0.5800                 0.4678                 0.4678
 IR Inten    --    31.1012                20.6161                20.6161

                      4                      5                      6
                     A1                     E                      E
 Frequencies --  1243.4844              1467.7334              1467.7334
 Red. masses --     1.1470                 1.0753                 1.0753
 Frc consts  --     1.0450                 1.3648                 1.3648
 IR Inten    --    91.6533                 4.0558                 4.0558

                      7                      8                      9
                     A1                     E                      E
 Frequencies --  3154.7590              3320.3268              3320.3268
 Red. masses --     1.0186                 1.1134                 1.1134
 Frc consts  --     5.9728                 7.2324                 7.2324
 IR Inten    --    20.3356                22.5187                22.5187


 -------------------
 - Thermochemistry -
 -------------------
 Temperature   298.150 Kelvin.  Pressure   1.00000 Atm.
 Atom     1 has atomic number 80 and mass 201.97060
 Atom     2 has atomic number  6 and mass  12.00000
 Atom     3 has atomic number  1 and mass   1.00783
 Atom     4 has atomic number  1 and mass   1.00783
 Atom     5 has atomic number  1 and mass   1.00783
 Molecular mass:   216.99408 amu.

Warning -- explicit consideration of   1 degrees of freedom as
           vibrations may cause significant error
 Vibrational temperatures:    632.26  1225.64  1225.64  1789.09  2111.74
          (Kelvin)           2111.74  4538.99  4777.20  4777.20


 Zero-point correction=                           0.036718 (Hartree/Particle)
 Thermal correction to Energy=                    0.039979
```

```
 Thermal correction to Enthalpy=                  0.040923
 Thermal correction to Gibbs Free Energy=         0.011323
 Sum of electronic and zero-point Energies=           -192.079919
 Sum of electronic and thermal Energies=              -192.076659
 Sum of electronic and thermal Enthalpies=            -192.075715
 Sum of electronic and thermal Free Energies=         -192.105315
==========================================================================

-------------------------------------------------------------
 #P CCSD-T(FC,MaxCyc=100) SCF(Tight) CHKbasis GEOM=allcheck
 -------------------------------------------------------------

                     CCSD(T)= -0.19214863861D+03

\St
 ate=1-A1\HF=-191.8405862\MP2=-192.1166373\MP3=-192.130343\MP4D=-192.13
 81961\MP4DQ=-192.135011\MP4SDQ=-192.1398528\CCSD=-192.1388403\CCSD(T)=
 -192.1486386

==========================================================================
```

Table SXXII. The data for the MP2-optimization of the complex $[CH_3–Hg–CH_3 \bullet OH]^-$ (CP-corrected energy).

```
---------------------------------------------------------------------
                            MP2:
---------------------------------------------------------------------
Counterpoise:    corrected energy =    -307.735253114686
 Counterpoise:        BSSE energy =       0.055519441251
---------------------------------------------------------------------

Harmonic frequencies (cm**-1), IR intensities (KM/Mole), Raman scattering
 activities (A**4/AMU), depolarization ratios for plane and unpolarized
 incident light, reduced masses (AMU), force constants (mDyne/A),
 and normal coordinates:
                      1                      2                      3
                      A                      A                      A
 Frequencies --    32.4564                56.4019               111.3483
 Red. masses --     1.0233                 1.0470                 3.9736
 Frc consts  --     0.0006                 0.0020                 0.0290
 IR Inten    --     0.0888                 0.4222                19.2207

                      4                      5                      6
                      A                      A                      A
 Frequencies --   129.1402               137.1807               285.5925
 Red. masses --     2.9150                 2.8404                 9.4092
 Frc consts  --     0.0286                 0.0315                 0.4522
 IR Inten    --     2.6741                 1.9253               115.3168

                      7                      8                      9
                      A                      A                      A
 Frequencies --   312.0567               484.3828               508.7158
 Red. masses --     1.0907                 3.7725                 3.9548
 Frc consts  --     0.0626                 0.5215                 0.6030
 IR Inten    --    64.0509                 3.6269                61.0564

                     10                     11                     12
                      A                      A                      A
 Frequencies --   576.8285               692.5412               742.4874
 Red. masses --     1.1028                 1.1422                 1.1743
 Frc consts  --     0.2162                 0.3228                 0.3814
 IR Inten    --    71.0530                 0.3125                 0.9517

                     13                     14                     15
                      A                      A                      A
 Frequencies --   772.7991               787.7427              1237.2210
 Red. masses --     1.2217                 1.2189                 1.2120
 Frc consts  --     0.4299                 0.4457                 1.0931
 IR Inten    --    50.2908                56.0225                 2.8748

                     16                     17                     18
                      A                      A                      A
 Frequencies --  1242.3815              1511.9525              1514.2493
 Red. masses --     1.2096                 1.0603                 1.0567
 Frc consts  --     1.1000                 1.4280                 1.4275
 IR Inten    --     2.0426                 1.0057                 0.8694
```

```
                     19                     20                     21
                      A                      A                      A
 Frequencies --   1518.7519              1519.7544              3106.7222
 Red. masses --      1.0605                 1.0636                 1.0318
 Frc consts  --      1.4412                 1.4473                 5.8673
 IR Inten    --      0.4163                 0.2967                62.4171

                     22                     23                     24
                      A                      A                      A
 Frequencies --   3110.5202              3194.8275              3201.8172
 Red. masses --      1.0324                 1.1003                 1.1008
 Frc consts  --      5.8852                 6.6167                 6.6489
 IR Inten    --     27.8349                47.0066                35.6529

                     25                     26                     27
                      A                      A                      A
 Frequencies --   3202.9716              3231.3755              3692.7297
 Red. masses --      1.1022                 1.1020                 1.0668
 Frc consts  --      6.6621                 6.7799                 8.5710
 IR Inten    --     46.7001                23.7411                145.3180


 -------------------
 - Thermochemistry -
 -------------------
 Temperature   298.150 Kelvin.  Pressure   1.00000 Atm.
 Atom     1 has atomic number 80 and mass 201.97060
 Atom     2 has atomic number  6 and mass  12.00000
 Atom     3 has atomic number  1 and mass   1.00783
 Atom     4 has atomic number  1 and mass   1.00783
 Atom     5 has atomic number  1 and mass   1.00783
 Atom     6 has atomic number  6 and mass  12.00000
 Atom     7 has atomic number  1 and mass   1.00783
 Atom     8 has atomic number  1 and mass   1.00783
 Atom     9 has atomic number  1 and mass   1.00783
 Atom    10 has atomic number  8 and mass  15.99491
 Atom    11 has atomic number  1 and mass   1.00783
 Molecular mass:   249.02029 amu.


Warning -- explicit consideration of  10 degrees of freedom as
           vibrations may cause significant error
 Vibrational temperatures:     46.70    81.15   160.21   185.80   197.37
          (Kelvin)            410.90   448.98   696.92   731.93   829.93
                              996.41  1068.27  1111.88  1133.38  1780.08
                             1787.51  2175.36  2178.66  2185.14  2186.58
                             4469.87  4475.34  4596.64  4606.70  4608.36
                             4649.22  5313.01

 Zero-point correction=                           0.084098 (Hartree/Particle)
 Thermal correction to Energy=                    0.092583
 Thermal correction to Enthalpy=                  0.093527
 Thermal correction to Gibbs Free Energy=         0.048759
 Sum of electronic and zero-point Energies=           -307.651155
 Sum of electronic and thermal Energies=              -307.642670
 Sum of electronic and thermal Enthalpies=            -307.641726
 Sum of electronic and thermal Free Energies=         -307.686494
```

Table SXXIII. Pseudopotential (MDF60) parameters used in the present study for Hg.

Pseudopotential Parameters							
Center	Atomic Number	Valence Electrons	Angular Momentum	Power of R	Exponent	Coefficient	SO-Coeffient
Hg	80	20					
			H and up				
				2	1.0000000	0.00000000	0.00000000
			S - H				
				2	12.9815490	274.53216900	0.00000000
				2	6.4907740	49.18219200	0.00000000
			P - H				
				2	10.5380960	237.39577000	0.00000000
				2	5.2690480	28.12158400	0.00000000
			D - H				
				2	8.1017210	114.25203400	0.00000000
				2	4.0508600	18.49563800	0.00000000
			F - H				
				2	3.8857910	30.36499600	0.00000000
			G - H				
				2	6.2410000	-29.47311800	0.00000000

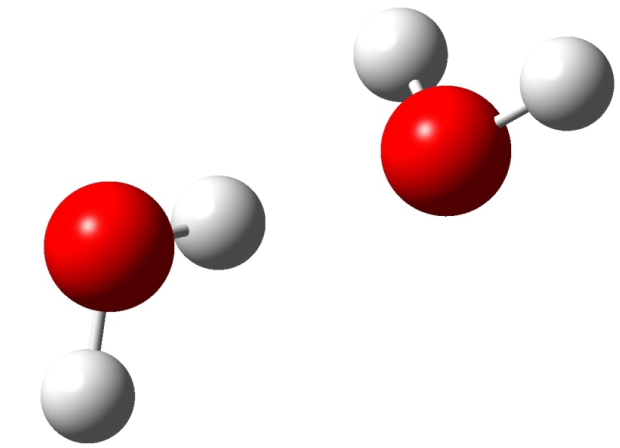

(A) **$H_2O \bullet H_2O$**

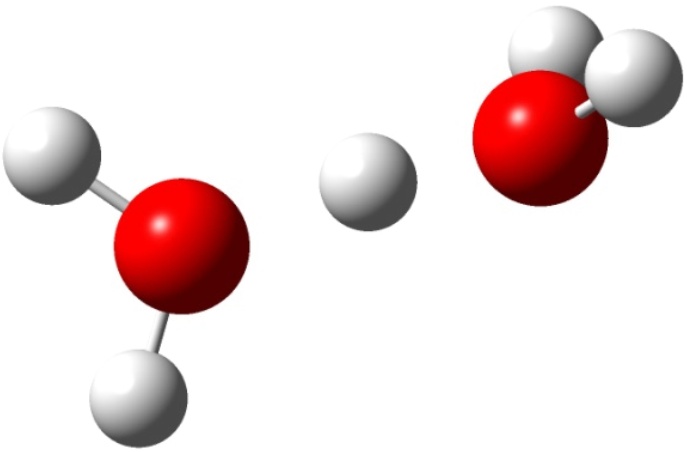

(B) **$H_5O_2^+$**

Figure S1. Optimized geometries for water dimer (panel A) and Zundel ion $H_5O_2^+$(panel B).

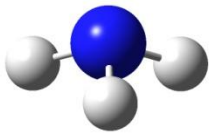

(A) NH_3

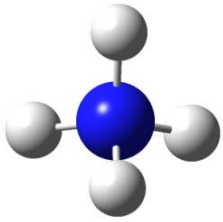

(B) **NH_4^+**

Figure S2. Optimized structures for NH_3 (panel A) and NH_4^+ (panel B).

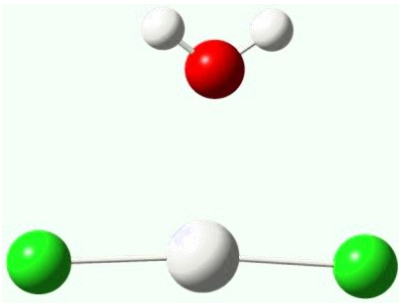

(A) Cl-Hg-Cl • H_2O

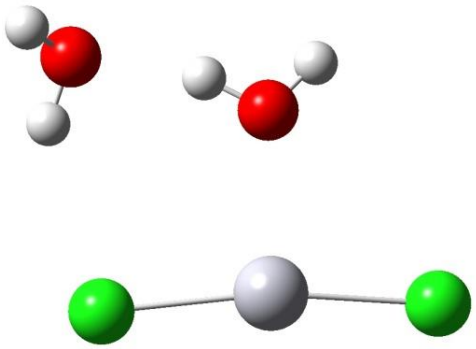

(B) Cl-Hg-Cl•(H_2O-H_2O)

Figure S3. Comparison of the bound complexes resulting from the interaction of Cl-Hg-Cl with H_2O (panel A) and H_2O-OH_2 (panel B).